

Fractal Dimension of Breast Cancer Cell Migration in a Wound Healing Assay

R. Sullivan, T. Holden, G. Tremberger, Jr, E. Cheung, C. Branch, J. Burrero, G. Surpris, S. Quintana, A. Rameau, N. Gadura, H. Yao, R. Subramaniam, P. Schneider, S. A. Rotenberg, P. Marchese, A. Flamholz, D. Lieberman, and T. Cheung

Abstract—Migration in breast cancer cell wound healing assay had been studied using image fractal dimension analysis. The migration of MDA-MB-231 cells (highly motile) in a wound healing assay was captured using time-lapse phase contrast video microscopy and compared to MDA-MB-468 cell migration (moderately motile). The Higuchi fractal method was used to compute the fractal dimension of the image intensity fluctuation along a single pixel width region parallel to the wound. The near-wound region fractal dimension was found to decrease three times faster in the MDA-MB-231 cells initially as compared to the less cancerous MDA-MB-468 cells. The inner region fractal dimension was found to be fairly constant for both cell types in time and suggests a wound influence range of about 15 cell layer. The box-counting fractal dimension method was also used to study region of interest (ROI). The MDA-MB-468 ROI area fractal dimension was found to decrease continuously up to 7 hours. The MDA-MB-231 ROI area fractal dimension was found to increase and is consistent with the behavior of a HGF-treated MDA-MB-231 wound healing assay posted in the public domain. A fractal dimension based capacity index has been formulated to quantify the invasiveness of the MDA-MB-231 cells in the perpendicular-to-wound direction. Our results suggest that image intensity fluctuation fractal dimension analysis can be used as a tool to quantify cell migration in terms of cancer severity and treatment responses.

Keywords—Higuchi fractal dimension, box-counting fractal dimension, cancer cell migration, wound healing.

I. INTRODUCTION

CELL migration is a complex process that plays a role in many physiological and disease systems including wound healing, embryogenesis, maintenance of glands and tumor formation. Although many assays have been developed to study cell migration the details of the process are not fully

understood. In vitro scratch assay has been used for over twenty years to study cell migration. The influence of COX-2 rate-limiting enzyme using MDA-MB-231 wound migration assay has been reported [1, 2]. The scratch assay is well-suited to study cell-cell interactions and cell-ECM interactions. The high molecular mass hyaluronan acting as a soluble chemo-attractant was found to be promoting the directional migration of MDA-MB-468 and MDA-MB-231 breast cancer cells [3]. Besides chemical influence, electrical de-polarization of tumor epithelial cells can also affect migration. The MDA-MB-231 cells were found to respond to applied electric fields with strong directional migration towards the anode [4]. The lack of telopeptides in fibrillar collagen polymerization also was found to promote the invasion of MDA-MB-231 cells [5]. It has been demonstrated in invasion assays that MDA-231 cell invasion is proportional to the levels of endogenous p120 catenin and the data also suggests that endogenous p120 mediates hepatocyte-growth-factor-induced migration [6]. All of these studied migration images contain intensity fluctuation that can be further analyzed for additional information. Fractal nature of cell colonies was reported to be similar with molecular beam epitaxy dynamics [7].

This study was undertaken to determine if fractal analysis would be an appropriate method for the measurement of the migration of human breast cancer cell lines. Fractal analysis determines the extent of randomness in a system. This type of analysis will allow for comparison of coordinated cell migration under different conditions such as type and concentration of attachment substrate. The migration of MDA-MB-231 cells (highly motile and invasive) in a wound healing assay was captured using time-lapse phase contrast video microscopy over different time scales, and compared to MDA-MB-468 cells (moderately motile). The fractal dimension difference for the images can be ascribed to cell reorientation under the influence of the neighboring cells. The macroscopic movement of the wound in time was found to correlate with the time dependent fractal dimension suggesting that the local cell reorientation controlled the healing. The effects of sulforaphane on cell growth and death in MDA-MB 231 and MDA-MB-468 have been reported [8]. An established fractal dimension algorithm for wound healing assay application can be used for therapy-related studies as well.

R. Sullivan, R. Subramaniam, C. Branch, J. Burrero, G. Surpris, S. Quintana, A. Rameau, N. Gadura, and P. Schneider are with CUNY Queensborough Community College, Biology Department, Bayside, NY 11364 USA (corresponding author: Regina Sullivan email: rsullivan@qcc.cuny.edu).

T. Holden, G. Tremberger, Jr, E. Cheung, P. Marchese, A. Flamholz, T. Cheung, and D. Lieberman are with CUNY Queensborough Community College, Physics Department, Bayside, NY 11364 USA (corresponding authors: Todd Holden, email: tholden@qcc.cuny.edu, David Lieberman, email: dlieberman@qcc.cuny.edu).

H. Yao is with CUNY Queensborough Community College, Mathematics Department, Bayside, NY 11364 USA.

S. A. Rotenberg is with CUNY Queens College, Biochemistry Department, Flushing, NY 11367 USA.

II. MATERIALS & METHODS

A. Wound Healing Assays

Live breast cancer cell (MDA-MD-231 and MDA-MB-468) samples were harvested from standard cultures. The cells were cultured in Iscove medium supplemented with 5% equine serum, 100µg/ml penicillin/streptomycin and 0.5µg/ml fungizone. All solutions were purchased from Gibco, USA. Both cell lines were maintained at 37°C and 5% CO₂. Cells are plated on 60mm and grown to a confluent monolayer. The “scratch” was introduced by scraping the monolayer with a p200 pipette tip [9]. The images were acquired using a MicroFire camera fitted to a Zeiss Inverted Phase Microscope.

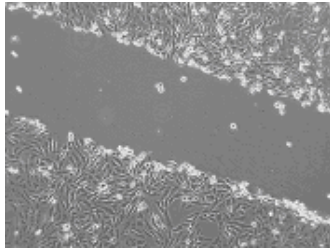


Fig. 1 A typical wound healing assay of MBA-MD-231 (400 micron x 300 micron)

B. Higuchi Fractal Method

Among the various fractal dimension methods, the Higuchi fractal method is well suited for studying signal fluctuation in one dimension [10]. The image intensity forms a data series called I . The numerical sequence I could be used to generate a difference series $(I(j)-I(i))$ for different lags. The non-normalized apparent length of the series curve is simply $L(k) = \sum \text{absolute } (I(j)-I(i))$ for all $(j-i)$ pairs that equal to k . The number of terms in a k -series varies and normalization must be used. The normalization is in open literature [11]. If the $I(i)$ is a fractal function, then the $\log(L(k))$ versus $\log(1/k)$ should be a straight line with the slope equal to the fractal dimension. Sometimes $\ln(L(k))$ vs $\ln(1/k)$ can be used as well [12]. Higuchi incorporated a calibration division step (divided by k) such that the maximum theoretical value is calibrated to the topological value of 2. When comparing the dimension of two fractal forms, the popular method of taking the difference of the two Higuchi fractal dimension values is valid within a constant regardless of the calibration division step. The Higuchi fractal algorithm used in this project was calibrated with the Weierstrass function. This function has the form $W(x) = \sum a^{-nh} \cos(2\pi a^n x)$ for all the n values 0, 1, 2, 3... The fractal dimension of the Weierstrass function was given by $(2 - h)$ where h takes on an arbitrary value between zero and one. Whether a data series is truly a fractal object when fractal dimension value is extractable can still be a debatable issue for the sake of finding the truth. The pragmatic approach was taken in that when the Higuchi fractal algorithm extracts a fractal dimension with a good R-square value of the log-log graph, then the image can be treated as a fractal object as far as application is concerned. The issue of multi-fractal is another possibility when another regression can be performed with a different set of $\log(1/k)$ values away

from the origin. This project calculated the regression slope by using the first seven points. The issue of multi-fractal, although interesting, is outside the current scope of this project. A Gaussian noise data series usually has a fractal dimension around 2. A short series (1000 or less) can have fractal dimension exceeding 2. A typical fractal curve is shown in Fig. 1 and the slope was computed using the first seven data points. A unity amplitude sine signal usually has a fractal dimension of about 1.

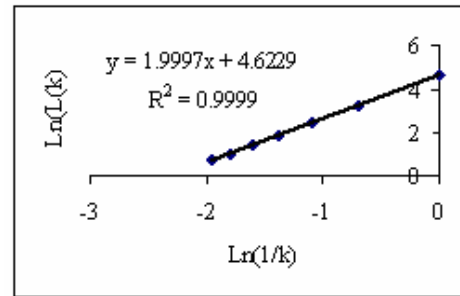


Fig. 2 Fractal curve of Gaussian (0, 0.1). The series had 1000 data points

III. RESULTS AND DISCUSSION

A. Fractal Analysis

The intensity versus distance data series from a typical linear digitization is shown in Fig. 3.

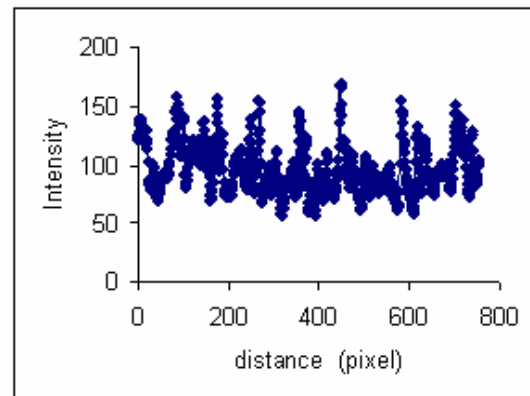


Fig. 3 Intensity versus distance of a typical linear digitization data series (1 micron ~ 4 pixels)

The corresponding fractal curve is shown in Fig. 4.

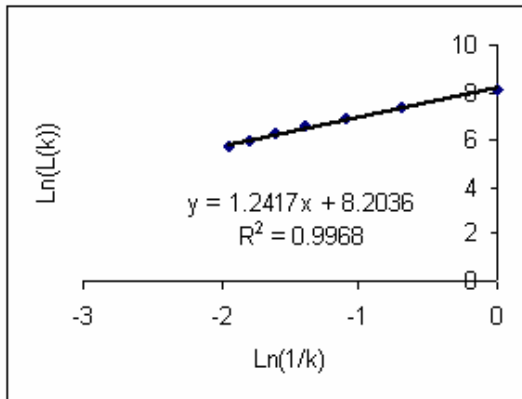


Fig. 4 Fractal dimension curve of the data series in Fig. 3

The fractal dimension calculations were performed for a near-wound single-pixel-width region at a fix distance from the wound. The digitization direction is parallel to the wound direction. The linear digitization of each image at different time was performed and the fractal dimension calculated. The results are displayed in Fig. 5. The overall fractal dimension change is about 0.1 for MDA-MB-231 and 0.05 for MDA-MB-468. The initial fractal dimension change of MDA-MB-231 is about three times faster than that of MDA-MB-468. The result is consistent with the highly invasive nature of MDA-MB-231.

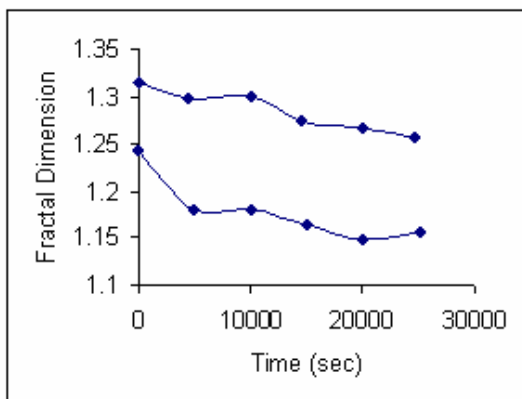


Fig. 5 Fractal dimension versus time for a near-wound single-pixel-width region linear digitization. The upper curve is MDA-MB-468 and the lower curve is MDA-MB-231

Similar analysis was performed for an inner region about 15 cell layers away from the wound (Fig. 6). The inner region fractal dimension was found to be fairly constant for both cell types in time and suggests the wound has no influence at the range of about 15 cell layer.

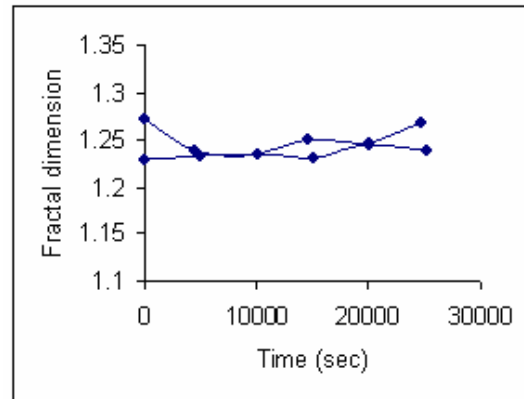


Fig. 6 Fractal dimension versus time for an inner region linear digitization. The upper curve is MDA-MB-468 and the lower curve is MDA-MB-231. (The scale is the same as in Fig. 5 for easy comparison and there is no cross over near the end)

B. Box Counting Fractal Dimension

The box-counting fractal dimension method was also used to study region of interest (ROI). The ImageJ software was used in our analysis. This software has been maintained by the US National Institutes of Health and is available for free download from the internet. It was reported in a previous WASET presentation that the ImageJ fractal dimension procedure has an error of about 2% in the calculation of the Sierpinski Gasket [13]. The box counting fractal dimension variation over time is displayed in Fig. 7. The ROI has a dimension of 350 pixel x 750 pixel near the wound.

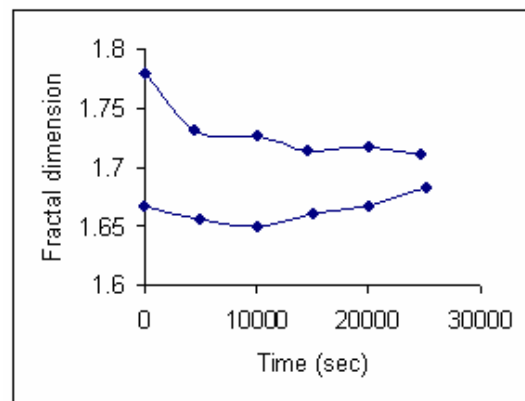


Fig. 7 Box-counting fractal dimension versus time. The upper curve is MDA-MB-468 and the lower curve is MDA-MB-231

The box-counting fractal dimension of the MDA-MB-468 migration ROI area fractal dimension decreases like the Higuchi fractal dimension method findings in Fig. 5. However, it is rather peculiar that the box-counting fractal dimension of the MDA-MB-231 migration increases in contrast to the Higuchi fractal dimension method findings in Fig. 5. The cell-cell interaction in the direction perpendicular to the wound cannot be further studied by the Higuchi fractal dimension method because the number of data points is

limited. The fact remains that MDA-MB-231 cell migration has an extra feature as revealed by the area fractal dimension.

The MDA-MB-231 ROI area fractal dimension was found to increase after 7 hours and is consistent with the behavior of a HGF-treated MDA-MB-231 wound healing assay posted in the public domain. The US Mayo Clinic posted a data video of such a migration [14]. The displayed ROI area fractal dimension calculation (box-counting) was performed on an area of 33 pixel x 235 pixels on the left of a video frame. The ROI was selected a few cell layers away from the wound so that a confluent region was analyzed. The result is displayed in Fig. 8. The time of 0.5 unit in Fig. 8 corresponds to about 7 hours in Fig. 7 judging from the width of the wound. A fractal dimension of about 2 usually can be interpreted as having an underlying Gaussian distribution (Fig. 1). The assumption of Gaussian statistics may not be correct for the wound assay intensities. The addition of uniformly distributed variables would generate a Gaussian distribution while taking the tangent of a uniformly distributed variable would generate a Cauchy-Lorentz distribution with long tail-ness. Taking the sine of a uniformly distributed variable would generate a distribution that goes as the inverse of the square root of $(1 - x^2)$, to within a constant such that the area of the curve is one. The rather low fractal dimension of the intensity fluctuation in the area fractal dimension and Higuchi fractal dimension suggests a long tail-ness feature in the underlying statistical distribution.

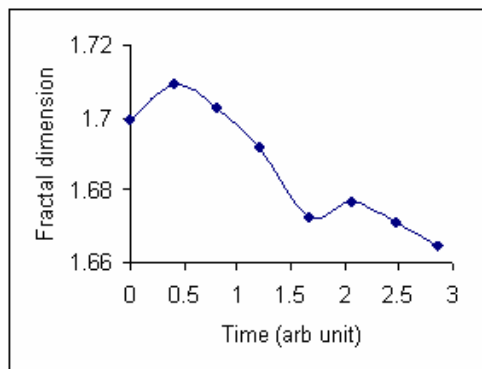


Fig. 8 Box-counting fractal dimension versus time for the data video of MDA-MB-231 of Reference 14

The intensity or brightness fluctuation in a 2-dim image can also be studied via its standard deviation. The brightness standard variation over time is shown in Fig. 9.

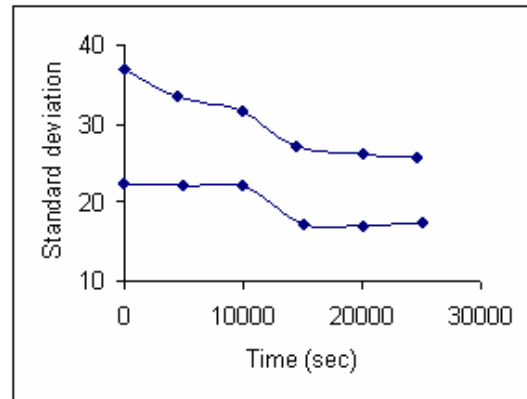


Fig. 9 The brightness standard deviation of the studied ROI in Fig. 7. The upper curve is MDA-MB-468 and the lower curve is MDA-MB-231

For comparison, the change of the coefficient of variation (CV) over time is displayed in Fig. 10. The CV parameter, being the standard deviation normalized by the average, is generally considered as a better measure of dispersion in a distribution or histogram. Upon normalization, the MDA-MB-468 CV variation in Fig. 10 upper curve is less pronounced as compared to the standard deviation variation in Fig. 9 upper curve. The MDA-MB-231 standard deviation and CV variations suggested less fluctuation over time but yet the area fractal dimension is increasing in Fig. 7 lower curve of MDA-MB-231. Furthermore, the apparent drop of standard deviation (Fig. 9 lower curve) and CV (Fig. 10 lower curve) near $T \sim 10,000$ sec for MDA-MB-231 and the coincidental increase of the box-counting fractal dimension (Fig. 7 lower curve) at the same time scale may not be related. One must bear in mind that standard deviation is position independent while fractal dimension is position sensitive. A cell rotation may not have affected the standard deviation but the fractal dimension can certainly change.

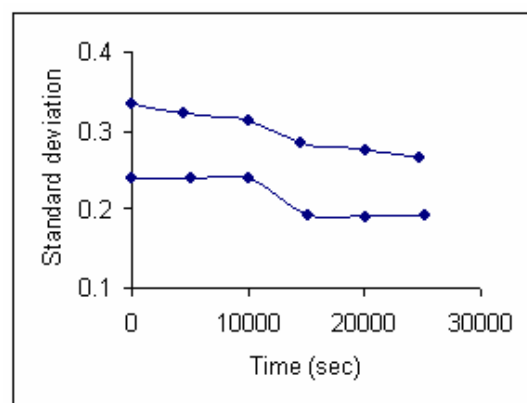


Fig. 10 The brightness coefficient of variation of the studied ROI in Figure 7. The upper curve is MDA-MB-468 and the lower curve is MDA-MB-231

The study of the invasiveness of MDA-MB-231 in the direction perpendicular to the wound requires a different modeling as the short perpendicular data series does not render a Higuchi fractal dimension calculation. Fractal dimension can be interpreted as a measure of the capacity dimension, which is the upper bound for information dimension [15]. The parallel direction capacity dimension is mixed with the perpendicular direction capacity dimension to yield a 2-dim capacity dimension. Operationally it can be interpreted as the Higuchi fractal dimensions in x and y directions being mixed together to yield an area fractal dimension. A perpendicular capacity index can be formulated via the ratio of area fractal dimension to the average 1-dim Higuchi fractal dimension in the parallel direction. The result is displayed in Fig. 11.

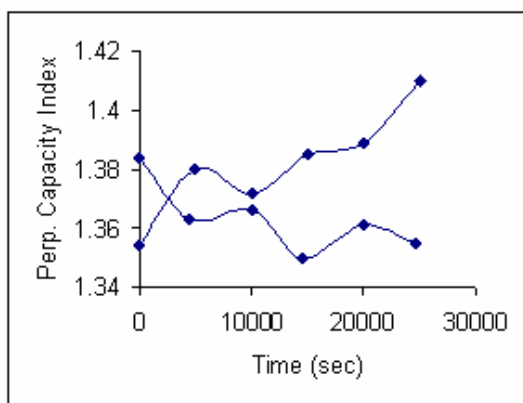


Fig. 11 The perpendicular capacity index versus time variation. The MDA-MB-468 curve starts at 1.384 and the MDA-MB-231 curve starts at 1.354. There is a cross over at ~ 2,500 sec

The perpendicular capacity index increases by about 0.07 for MDA-MB-231 and decreases by about 0.03 for MDA-MB-468. The continuous increase of perpendicular capacity index at time ~ 10,000 sec and the apparent abrupt change at the same time scale for the brightness standard deviation (Fig. 9 lower curve) and CV (Fig. 10 lower curve) suggest the onset of control pathway(s) unique to the MDA-MB-231 cells.

On the whole, our results suggest that image intensity fluctuation fractal dimension analysis can be used as a tool to quantify cell migration in terms of cancer severity and treatment responses.

IV. CONCLUSION

This project has demonstrated that fractal analysis can be used to study the migration of breast cancer cell in a wound healing assay. The fractal dimension calculation was able to give a quantitative description of the migration. The near-wound region fractal dimension was found to decrease three times faster in the MDA-MB-231 cells initially as compared to the less invasive MDA-MB-468 cells. The box-counting fractal dimension method was also used to study region of interest (ROI). The MDA-MB-468 ROI area fractal dimension was found to decrease continuously up to 7 hours. The MDA-MB-231 ROI area fractal dimension was found to increase and is consistent with the behavior of a HGF-treated MDA-

MB-231 wound healing assay posted in the public domain. A perpendicular capacity index has been formulated via the ratio of area fractal dimension to the average 1-dim Higuchi fractal dimension in the parallel direction. An onset of a continuous increase of the perpendicular capacity index in MDA-MB-231 cell migration was observed and is interpreted as control pathway related. The detailed interaction of the parallel-to-wound fractal dimension with the area fractal dimension would be an interesting future study.

ACKNOWLEDGMENT

The project was partially supported by several CUNY PSC and Collaborative grants. A.F. and R. Sullivan received partial support from CUNY New Faculty Programs. E.C. thanks the hospitality of QCC. C.B., J.B., G.S., S.Q., and A.R. thank QCC for their student stipend support made possible by a NIH grant (PI: P. Schneider). We thank J. Spinella for helping us in the microscopy work. We thank the Mayo Clinic Florida Cell Adhesion and Metastasis Lab (PI: Panagiotis. Anastasiadis PhD) for posting their video data in the public domain.

REFERENCES

- [1] Teri L Larkins, Marche Nowell, Shailesh Singh and Gary L Sanford, "Inhibition of cyclooxygenase-2 decreases breast cancer cell motility, invasion and matrix metalloproteinase expression" *BMC Cancer*, Vol 6, p181-193, doi:10.1186/1471-2407-6-181, 2006.
- [2] Gargi D Basu, Latha B Pathangay, Teresa L Tindler, Sandra J Gendler and Pinku Mukherjee, "Mechanisms underlying the growth inhibitory effects of the cyclo-oxygenase-2 inhibitor celecoxib in human breast cancer cells" *Breast Cancer Research*, Vol. 7, R422-R435, 2005.
- [3] George Tziricotis, Rick F. Thorne and Clare M. Isacke, "Chemotaxis towards hyaluronan is dependent on CD44 expression and modulated by cell type variation in CD44 hyaluronan binding" *Journal of Cell Science* Vol. 118, p5119-5128, 2005.
- [4] Jin Pu, Colin D. McCaig, Lin Cao, Zhiqiang Zhao, Jeffrey E. Segall and Min Zhao, "EGF receptor signalling is essential for electric-field directed migration of breast cancer cells" *Journal of Cell Science* Vol. 120, p3395-3403, 2007.
- [5] Zoe N. Demou, Michael Awad, Trevor McKee, Jean Yannis Perentes, Xiaoye Wang, Lance L. Munn, Rakesh K. Jain, and Yves Boucher, "Lack of Telopeptides in Fibrillar Collagen I Promotes the Invasion of a Metastatic Breast Tumor Cell Line" *Cancer Research* Vol. 65: p5674-5682, 2005.
- [6] Masahiro Yanagisawa and Panos Z. Anastasiadis, "p120 catenin is essential for mesenchymal cadherin-mediated regulation of cell motility and invasiveness" *The Journal of Cell Biology*, Vol. 174, p1087-1096, 2006.
- [7] A. Bru, S. Albertos, J. Subiza, J. Garcia-Asenjo, and I. Bru, "The Universal Dynamics of Tumor Growth" *Biophysical Journal*, vol-85, 2948-2961, 2003.
- [8] Allison Pledgie-Tracy, Michele D. Sobolewski, and Nancy E. Davidson, "Sulforaphane induces cell type-specific apoptosis in human breast cancer cell lines" *Mol Cancer Ther* Vol. 6, p1013-1021, 2007.
- [9] Liang C. et al., "In vitro scratch assay: a convenient and inexpensive method for analysis of cell migration in vitro *Nature protocols* 2; (<http://www.nature.com/nature/protocol>), 2007.
- [10] W. Klonowski "From conformons to human brains: an informal overview of nonlinear dynamics and its applications in biomedicine". *Nonlinear Biomed Phys.* 2007 Jul 5; 1(1):5.
- [11] T. Higuchi, "Approach to an irregular time series on the basis of fractal theory", *Physica D*, vol 31, 277-283, 1998.
- [12] Xinmin Yang, Haluk Beyenal, Gary Harkin, Zbigniew Lewandowski, "Quantifying biofilm structure using image analysis", *Journal of Microbiological Methods*, Vol 39, Pages 109-119, 2000.

- [13] T. Sungkaworn, W. Triampo, P. Nalakarn, D. Triampo, I. M. Tang, Y. Lenbury, and P. Picha, "The Effects of TiO₂ Nanoparticles on Tumor Cell Colonies: Fractal Dimension and Morphological Properties" International Journal of Biomedical Sciences Vol. 2, p67-74, 2007.
- [14] http://mayoresearch.mayo.edu/mayo/research/anastasiadis_lab/cell-migration.cfm (last assessed September 12 2008).
- [15] E.W. Weisstein, "Capacity Dimension." From MathWorld--A Wolfram Web Resource. <http://mathworld.wolfram.com/>